Chapter 7

Protein Hydrodynamics

STEPHEN E. HARDING

Protein: A Comprehensive Treatise
Volume 2, pages 271–305

ISBN: 1-55938-672-X

ABSTRACT

This article provides a pointer for the non-specialist to the various hydrodynamic methodologies available for the characterisation of the size, conformation in dilute solution and interaction properties of proteins. The virtue of combining data from different techniques is stressed, particularly in connection with conformation analysis and its associated uniqueness and hydration problems.

INTRODUCTION

Hydrodynamics provides the protein scientist with a powerful array of methodologies for investigating the mass, conformation, and interaction properties of proteins in solution conditions—conditions in which they largely function in vivo. These methods can also provide an important supporting role to the so-called "high-resolution" structural probes of X-ray crystallography and nuclear magnetic resonance. In the case of nuclear magnetic resonance, because of the high concentrations of mass/volume required to give satisfactory spectra, simple sedimentation velocity or equilibrium runs in the analytical ultracentrifuge can provide vital checks against any self-association behavior that can give rise to misinterpretation of the chemical shift or related spectra. Hydrodynamic methods are generally rapid and nondestructive: these particular features have not escaped the notice of people such as molecular biologists, who often have only very small amounts of material available. They can provide early "low-resolution" information on a macromolecular structure prior to detailed crystallographic or high-resolution nuclear magnetic resonance analysis. Or conversely, they can provide the finishing touches refining a crystallographic model to account for *dilute* solution behavior, especially in terms of *inter*molecular interaction phenomena (Schachman, 1989). The delicate *intra*molecular relationships between subunits of a multienzyme complex can also be explored. In work now almost considered classical, H. K. Schachman and coworkers (Schachman et al, 1984) showed, using a combination of high-precision analytical ultracentrifuge measurements with the tools of molecular biology (production of point mutants) how such interactions in aspartate transcarbamoylase produce powerful allostery.

There have been many classic reviews on the application of hydrodynamic probes. Despite its age, C. Tanford's book (1961) is still regarded by many as the authority on the subject, although the subject has advanced considerably since that time particularly in terms of molecular weight and molecular weight distribution analysis, analysis of interaction parameters, and hydrodynamic conformation modelling (tri-axial ellipsoids, bead models, flexible particle analysis, etc.). The purpose of this article is thus to attempt to indicate some of the "late 1990's" state-of-the-art of hydrodynamic methodology for the investigation of macromolecular conformation in dilute solution. This article, with the general protein scientist in mind, will

not give a comprehensive review of the theory, experimentation, and applications of all hydrodynamic methodologies, but aims to provide a pointer to the various methodologies, and for each of the two classes of hydrodynamic measurement—mass and shape analysis—it will focus on certain techniques in more detail than others (this is merely a result of the particular expertise of the author). For example, for mass analysis, we focus on gel filtration and size exclusion chromatography (including on-line coupling with multiangle laser light scattering), dynamic light scattering, sedimentation velocity, and sedimentation equilibrium in the analytical ultracentrifuge. For shape measurement, we focus on sedimentation velocity and dynamic light scattering again, together with intrinsic viscosity, steady-state fluorescence depolarization, and the use of concentration dependence parameters, combined shape functions, and the radius of gyration. The treatment given here is by no means comprehensive, but certain key follow-up references will be given.

HYDRODYNAMIC TECHNIQUES

By "hydrodynamic" (Greek for "water-movement") techniques, we mean any technique involving motion of a macromolecule with, or relative to, the aqueous solvent in which it is dissolved or suspended. This therefore includes not only gel filtration and size-exclusion chromatography, viscometry, sedimentation (velocity and equilibrium), and rotational diffusion probes (fluorescence anisotropy depolarization and electric-optical methods) but also "classical" and "dynamic" light scattering that both (even "classical") derive from the relative motions of the (macromolecular) solute in relation to the solvent. Although this definition technically *also* includes electrophoretic methods, these will not be considered here. Let it suffice to say here however that electrophoretic methods, besides being powerful tools for separation, purification, and identification of proteins, can also, with "SDS" methodology, be used to provide an estimate of polypeptide molecular weight. Careful use of cross-linking agents can also give an indication of quaternary structure, although correct application of other hydrodynamic methods give a more precise picture.

This article therefore considers the hydrodynamic determination of molecular weight, or "molar mass", and quaternary structure (subunit composition and arrangement, self-association phenomena, and polydispersity). We will also consider the measurement of protein conformation in dilute solution.

MOLAR MASS (MOLECULAR WEIGHT) AND QUATERNARY STRUCTURE

For an *unglycosylated* polypeptide, a value to ±1 g/mol can be obtained from sequence information or from mass spectrometry . A similar precision cannot be obtained for glycosylated proteins because of polydispersity deriving from the variability of a cell's glycosylation process. Many proteins—and glycoproteins—

contain more than one noncovalently linked protein chain, particularly at higher concentrations, and important roles of hydrodynamic methods for mass analysis in protein chemistry are to give the molar mass of the "intact" or "quaternary" structure and to provide an idea of the strength of binding of these noncovalent entities through measurement of association constants.

Gel Filtration and Size Exclusion Chromatography

The simplest hydrodynamic method for measuring molar mass is gel filtration (Ackers, 1975), commonly referred to as "gel permeation chromatography" or now "size exclusion chromatography" since the chemical intertness of the separation medium is assumed. This was originally conceived as a method for the separation and purification of macromolecules but has developed over the years in its "calibrated" form as a very popular method for measuring protein molar masses both in native and dissociative conditions.

The separation medium of this method is a crosslinked gel. Traditionally, this has been made by using cross-linked polysaccharide or polyacrylamide beads and allowing them to swell in water; this is then packed into a glass or metal walled column, which is then equilibrated with the buffer in which the macromolecules to be separated are dissolved. Control of the degree of crosslinking will dictate the separation range of the gel: looser gels will separate larger molecules. Proper packing of columns requires some skill, and the user manuals as supplied by the commercial manufacturers are usually very comprehensive. The availability of prepacked, metal-walled columns for use in so-called "high-pressure" or "high-performance liquid chromatography" (HPLC) with positive pressure applied upstream of the column to accelerate the separation process makes the measurement particularly attractive for protein chemists.

Gel filtration or size exclusion chromatography depends on the principle that some of the space inside the gel particle is available to smaller molecules but unavailable to larger molecules that are excluded. Thus, when a solution is applied to the top of a properly packed gel column, only the dead space between gel particles is available to the excluded molecules, which therefore come off first when "elution" is commenced (addition of the buffer at a continuous rate, or equivalently with HPLC, injection of the solution into an already continuously running buffer system). The excluded molecules—the larger molecules—will thus have a smaller elution volume, V_e, and will elute first from the column. Smaller macromolecules, having progressively more and more space available to them as molar mass decreases, are accordingly eluted only at higher values of V_e. "Biggest come off the column first" is the rule of thumb for size exclusion chromatography. The separation is sometimes given in terms of the partition coefficient, K_{av} as defined by

$$V_e = V_o + K_{av}(V_t - V_o) \quad (1)$$

where V_o and V_t are the void volume and total volume of the column, respectively, determined from separate elutions using solute species having partition coefficients

of 0 (totally excluded) and 1 (non-excluded), respectively. Elution of proteins as they emerge from the column is monitored by the use of a spectrophotometer set for either 280 nm in the uv (trp and tyr residue absorption) or the more sensitive far-uv (210–230 nm-peptide bond), provided the buffer is reasonably transparent in the selected region. Reagents like ATP, azide, and so forth in buffers can cause serious problems for detection by causing an effective uv blackout. In these cases, use of a differential refractometer instead of a spectrophotometer is appropriate. Highly sensitive differential refractometers are now available, which are now arguably more preferable generally as the detection method of choice. The broadness of a peak eluting from a column does not necessarily mean the component is polydisperse: it more probably is a likely result of diffusion effects.

Empirically, the volume at which a protein elutes V_e and its molar mass M are related by the logarithmic expression (Ackers, 1975)

$$V_e = A - B \log_{10} M \tag{2}$$

where A and B are properties of the column. This equation is valid over the fractionation range of the gel and forms the basis of *calibrated gel chromatography* (Ackers, 1975): To obtain the molar mass of a protein molecule or mixture of

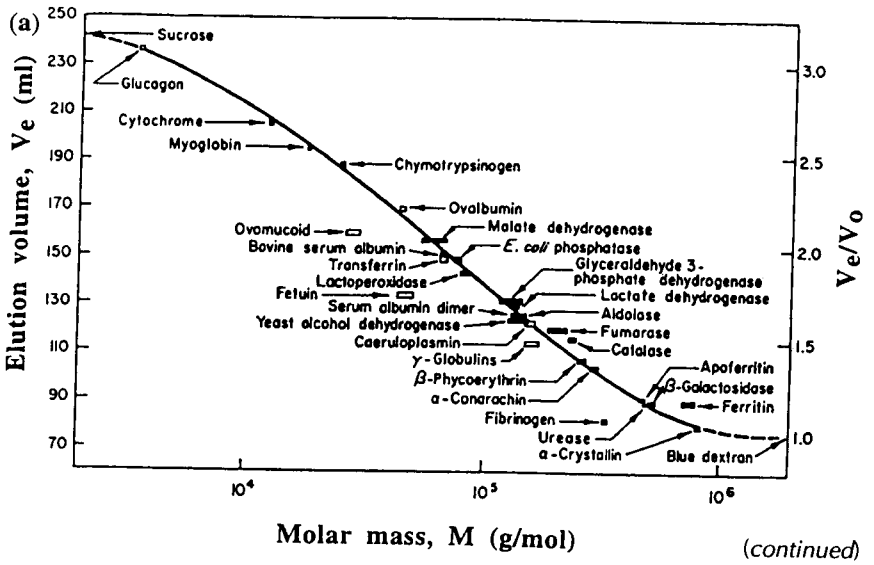

(*continued*)

Figure 1. Size exclusion chromatography. (**a**) SEC logarithmic calibration plot for proteins eluting from a Sephadex G-200 column. Reproduced with permission from Andrews (1965). (**b**) SEC elution volume/ molecular weight relation obtained directly from SEC/MALLS for a glycoprotein (pig gastric mucin, ≈80% glycosylated) (adapted from Jumel et al., 1996). (**c**) Molar mass distribution corresponding to (**b**).

(b)

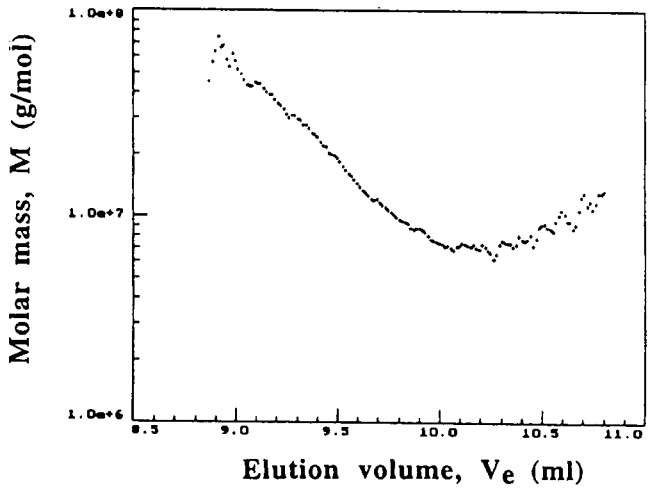

(c)

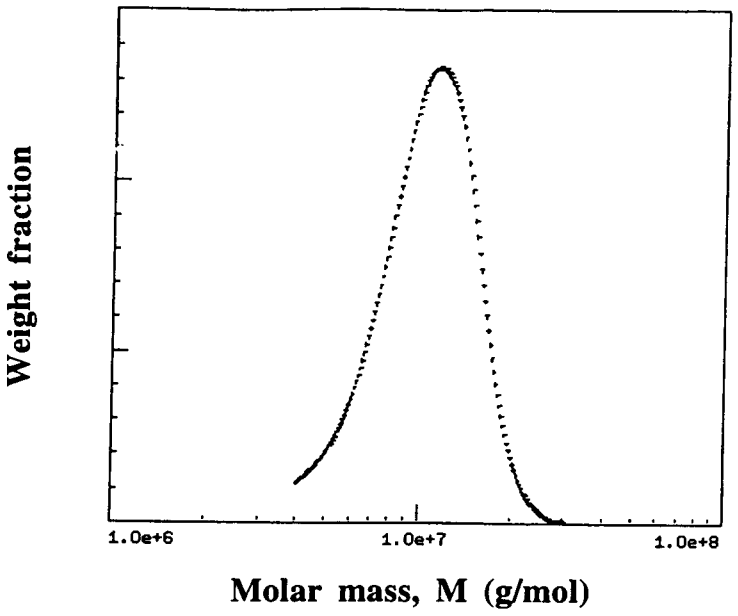

Figure 1. Continued

molecules, the column is first calibrated by the use of standard proteins or "markers" of known molar mass. Linear regression analysis is then used to evaluate A and B, and hence from the measured value of V_e of the unknown protein, M can be found. The calibration can only be applied within the gel's fractionation range, which will depend on the pore size (Figure 1a). Fractionation ability is normally enhanced by

running differing gel columns in series, a practice common with HPLC systems because of the much shorter elution times.

Equation 1 assumes the fractionation is based on the size-exclusion principle alone. Separation mechanisms not governed by the size of the molecules will tend to decouple the molecular size–migration velocity relation and the experimental elution profile will not reflect differences in size (Barth, 1980). Equation 1, which fails also outside the fractionation range of the gel, works only for molecules of similar shape and conformation. Thus calibration using globular protein standards would be inappropriate for fibrinogen and muscle proteins like myosin and titin (asymmetric) and also heavily glycosylated glycoproteins.

The theory behind equation 1 is not rigorous, but for globular proteins at least it seems to represent the data very well. For linear macromolecules of limited stiffness, there appears to be growing acceptance that the separation is more a logarithmic function of the hydrodynamic volume of a macromolecule ($\approx M \cdot [\eta]$ where $[\eta]$ is the intrinsic viscosity) and its corresponding hydrodynamic or "effective" radius r_H, culminating in a proposal for a "universal calibration" (Dubin and Principi, 1989). This may be more appropriate for proteins in denaturing solvents such as proteins in the presence of mercaptoethanol (disulfide bond breaker) and 6M GuHCl; for these substances, wider pore gels (e.g., sepharose) are a more appropriate separation medium.

These calibration problems can be avoided completely by coupling an absolute molar mass detector (a light scattering photometer) downstream from the column (Wyatt, 1992). This coupling, called "SEC/MALLS," is particularly valuable for the characterization of polydisperse heavily glycosylated protein systems such as mucus glycoproteins since it provides the elution volume to weight–average molar mass relationship without recourse to calibration standards (Figure 1b) and also provides the molar mass, or for a heterogeneous system, the molar mass distribution (Figure 1c) and its associated molar mass averages (number average, M_n, weight average, M_w, and z-average, M_z). The coupled light scattering and refractive index detectors are so sensitive that only low concentrations are required and problems through thermodynamic nonideality are usually negligible.

Dynamic Light Scattering (DLS)

Although the light scattering photometer described in the SEC/MALLS application above (often described as "static" light scattering) is not thought of as a classical "hydrodynamic" probe (although technically it is derived from motions of macromolecules relative to solvent), the technique of dynamic light scattering has without doubt a firm hydrodynamic basis and now appears to be the method of choice for the measurement of translational diffusion coefficients. In addition, via an approximation or by combination with sedimentation measurements, (see below) this method also provides an estimate for the molar mass. The appearance of simple-to-use, fixed- angle (90°) dynamic light scattering photometers has made dynamic

light scattering an increasingly popular tool amongst protein chemists. After certain assumptions and approximations, largely involving an assumed spherical shape, surprisingly reliable estimates for the molar mass of globular proteins have been obtained (Claes et al., 1992). When used in isolation, this method for molar mass measurement is, like gel filtration, *a relative one*, requiring a calibration using standard proteins of known molar mass. For asymmetric proteins like fibrinogen and myosin, the single-angle approximation fails, but extraction of molar mass and related parameters is still possible if multiangle instruments are used and the primary parameter, which comes from dynamic light scattering measurements, the translational diffusion coefficient D ($cm^2\ s^{-1}$), is combined with results from sedimentation analysis in the analytical ultracentrifuge (see below).

For a recent comprehensive treatment of the technique, the reader is referred to Brown's book (1995), and for a more introductory text, Schmitz (1990) and an article by Johnson (1984). Although the theory is complex, the principle of dynamic light scattering experiments is simple and is based on the high intensity, monochromaticity, collimation, and coherence of laser light. Laser light is directed onto a protein solution in a controlled temperature bath, and the intensity at either a single or multiple angles recorded using a photomultiplier/photodetector system. The

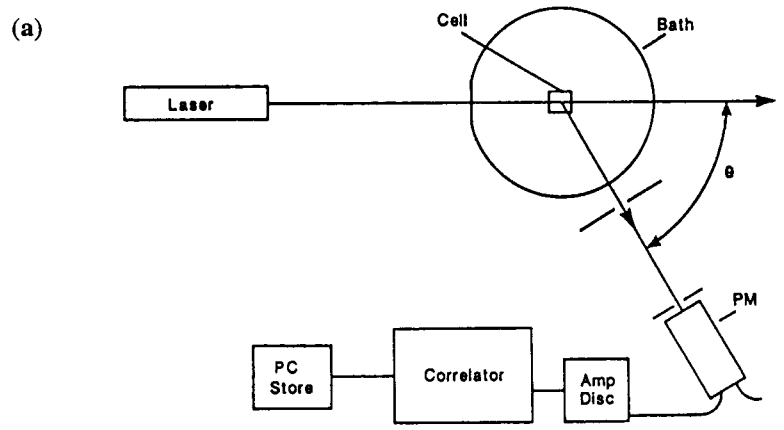

Figure 2. Dynamic light scattering. (**a**) Experimental set-up. (**b**) Normalized autocorrelation decay plot for the protein assembly Dynein (in 40 mM NaCl) $D^0_{20,w} = 1.1 \times 10^{-7}\ cm^2\ s^{-1}$; M (from equation 10) = 2.5×10^6 g/mol (adapted from Wells et al., 1990) (**c**)"MHKS" double-logarithmic calibration plot of r_H versus M : (1) thyroglobulin; (2) apoferritin; (3) IgG; (4) yeast alcohol dehydrogenase; (5) hexokinase; (6) amyloglucosidase; (7) horse alcohol dehydrogenase; (8) transferrin; (9) bovine serum albumin; (10) hemoglobin; (11) hexokinase subunit; (12) ovalbumin; (13) carbonic anhydrase; (14) chymotrypsinogen; (15) myoglobin; (16) lysozyme; (17) ribonuclease A. Reproduced with permission from Claes et al. (1992).

intensities recorded will fluctuate with time because of Brownian diffusive motions of the macromolecules; this movement causes a "Doppler" type of wavelength broadening of the otherwise monochromatic light incident on the protein molecules and the beating between waves of different but similar wavelength causes the intensity fluctuation. How rapid the intensity fluctuates (ns–μs time intervals)

(b)

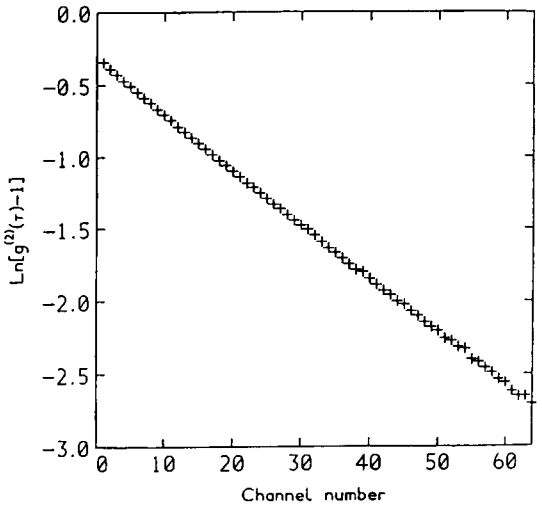

(c)

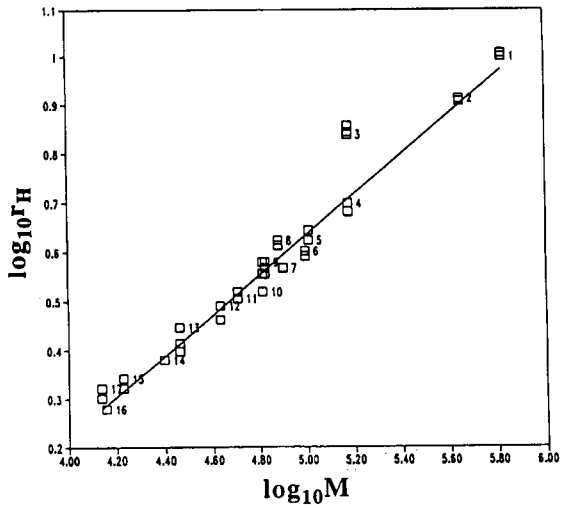

Figure 2. Continued

depends on the mobility or diffusivity of the protein molecules. A purpose-built computer called an autocorrelator, as indicated by its name, "correlates" or interprets these fluctuations. It does this by evaluating a "normalized intensity autocorrelation function," $g^{(2)}$, as a function of "delay time", "τ (ms–μs)". The decay of the correlation, $g^{(2)}(\tau)$, as a function of τ , averaged over longer time intervals (usually $\approx$ minutes) can then be used, by an interfaced PC (or the equivalent) to obtain D. (Larger and/or asymmetric particles that move more sluggishly will have slower intensity fluctuations, slower decay of $g^{(2)}$ (τ) with τ, and hence smaller D values compared to smaller and/or more globular particles). The delay time τ is itself the product of the "channel number" b (taking on all integral values between 1 and 64 or up to 128 or 256 depending on how expensive the correlator is) with a user-set "sample time", τ_s, (typically ~100 ns for a rapidly diffusing low molar mass [M ~ 20000 g/mol] enzyme, and increasing up to around milliseconds for microbes). In the past, τ_s was selected by trial and error, but now modern data-capture software usually does this automatically.

For spherical particles, a single term exponential describes the decay of Γ with τ:

$$g^{(2)}(\tau) - 1 = e^{-Dk^2\tau} \tag{3}$$

where k is the Bragg wave vector whose magnitude is defined by

$$k = \{4\pi n/\lambda\} \sin(\theta/2) \tag{4}$$

and where n is the refractive index of the medium, θ is the scattering angle, and λ (cm) is the wavelength of the incident light. Equation 3 can be reasonably applied to quasispherical particles like globular proteins or spheroidal protein assemblies (Figure 2b).

Fixed-Angle (90°) DLS Photometer

For globular proteins and spheroidal assemblies, application of equation 3 at only a single fixed angle is usually sufficient. Low angles are usually avoided because they magnify problems due to any contamination with dust or other supramolecular particles and thus an angle of 90° is normally used. For a given laser power at a given protein concentration, the smaller the protein the lower the intensity of scattered light and hence the longer the averaging required to give a sufficient signal. A commercial instrument is available based on this single fixed angle principle (Claes et al., 1992). To obtain molar mass information from D, a calibration curve of log D versus log M is produced (this is known as an "MHKS" {Mark-Houwink-Kuhn-Sakurada} relation; for example, see Harding, 1995) based on globular protein standards, and the approximation is made that this relation holds for the protein whose molar mass is being sought. Figure 2c shows such a calibration plot (The D values have been converted to hydrodynamic radius values, see below).

Other approximations and practical requirements with the operation of this type of fixed-angle instrument have to be made:

1. Solutions have to be as free as possible from dust and supramolecular aggregates. This requirement is met by injection of the sample into the (scrupulously clean) scattering cell via a millipore filter(s) of appropriate size (0.1–0.45 μm).
2. The diffusion coefficient is a sensitive function of temperature and the viscosity of the solvent (also sensitive to temperature) and the log D versus log M relationship must correspond to the same temperature.
3. The diffusion coefficient measured at a single concentration is an apparent one, D_{app}, because of nonideality effects (finite volume and charge). These effects become vanishingly small as the concentration $c \rightarrow 0$. The approximation which is usually reasonable for proteins, is made that $D_{app} \approx D$ *or* that nonideality effects are the same as for the calibration standards.

Despite these approximations, diffusion coefficients and molar masses obtained in this way with these fixed-angle instruments have been remarkably reliable. For nonglobular proteins, however both the log D versus log M calibration becomes invalid and also equation 3 no longer applies: an instrument with a multiangle facility must then be resorted to.

Multiangle Instruments

Measurements using multiangle equipment are more time-consuming and the instrumentation larger and more expensive. Data analysis is also more complicated. Equation 3 no longer applies largely because of the added complication of rotational diffusion effects. These effects vanish however as the scattering angle $\theta \rightarrow 0$. It is therefore possible to use equation 3 in terms of an apparent diffusion coefficient D_{app} with contributions from both concentration *and* rotational diffusion affects. D_{app} is measured at several angles and extrapolated back to zero angle to give D if concentration effects are negligible. However, if concentration dependence affects are suspected, then a double extrapolation can be performed on the same plot (called a "Dynamic Zimm plot") of D_{app} (or the equivalent autocorrelation function) to zero angle and zero concentration (Burchard, 1992). The common intercept gives the "ideal" (in a thermodynamic sense) diffusion coefficient, D^0. Because this quantity is not only an intrinsic property of the protein but also of the viscosity η(poise) and temperature T (K) of the buffer, it has to be corrected to standard conditions (viscosity of pure water at 20 °C, $\eta_{20,w}$) either before or after the extrapolation (van Holde, 1985) as shown in the following.

$$D^0_{20,w} = D^0 \cdot \{\eta/\eta_{20,w}\} \cdot \{T/293.15\} \tag{5}$$

The *size* of a protein, as represented by its equivalent hydrodynamic radius r_H, is related to $D^0_{20,w}$ by the Stokes equation according to the relation

$$r_H = k_B T/(6\pi\eta_{20,w} D^0_{20,w}) \tag{6}$$

where k_B is Boltzmann's constant. To obtain an absolute measure of *molar mass, M*, of a protein from $D^{\circ}_{20,w}$ without assumptions concerning the shape of the protein requires combination with the sedimentation coefficient from the analytical ultracentrifuge, as described below. Some modern software attempts to evaluate M directly from the diffusion coefficient; this should be treated with some caution.

For multiangle measurements, preferences vary in terms of the type of cuvets used. Square cuvets are optically more reliable, but cell corners obviously prohibit some scattering angles. Cylindrical cuvets, if used, should be of the wide diameter type (>2 cm) to avoid internal and stray reflections. Scrupulous attention to sample *and cuvet* clarity is mandatory, particularly for macromolecules of M<100000 g/mol, which give low scattering signals, and also if low angles are employed where the effects of supramolecular contaminants are at their maximum: special cuvet filling arrangements are used for clarification purposes (Sanders and Cannell, 1980). The angular extrapolation of D_{app} can provide an estimate for the rotational diffusion coefficient, albeit to a lower precision than conventional methods (fluorescence depolarization, electric birefringence). If the protein is polydisperse or self-associating, the logarithmic plot of the type shown in Figure 2b will tend to be curved, and the corresponding diffusion coefficient will be a z-average (Pusey, 1974) The spread of diffusion coefficients is indicated by a parameter known as the "Polydispersity Factor" (Pusey, 1974), which most software packages evaluate. Various computer packages are available from the commercial manufacturer for data capture and evaluation. In our laboratory, we prefer to capture the data in ASCII format using the data capture software of the commercial manufacturer and then to use our own in-house routine "PROTEPS" (Harding et al., 1997) or the evaluation of diffusion coefficients and polydispersity factors. More advanced routines are available, including "CONTIN", which was designed for the study of heterogeneous systems by going beyond the use of polydispersity factors and inverting the autocorrelation data directly to give distributions of particle size. These methods have been recently reviewed (Johnsen and Brown, 1992; Štepánek, 1993).

Dynamic light scattering is particularly valuable for the investigation of *changes* in macromolecular systems as long as the timescale of changes is of the order of minutes or hours, and not seconds or lower (Harding, 1986). Finally, it is worth pointing out that dynamic light scattering also provides a useful tool for monitoring electrophoretic mobilities (Langley, 1992) and commercial instrumentation is available for this purpose.

Sedimentation Velocity in the Analytical Ultracentrifuge

Combination of the sedimentation coefficient, s, from sedimentation velocity with the diffusion coefficient, D, from dynamic light scattering gives an absolute value for the molar mass of a protein without assumptions over conformation. This method for molar mass measurement was given by T. Svedberg (see Svedberg and Pedersen, 1940).

The basic principle of the technique is as follows: a solution of the protein is placed in a specially designed sector-shaped cell with transparent end windows. This in turn is placed in an appropriately balanced rotor and run in high vacuum at the appropriate speed (typically ≈ 50000–60000 rev/min for a protein of molar mass 10000–100000 g/mol, lower speeds for larger molecules). A light source positioned below the rotor transmits light via a monochromator or filter through the solution and a variety of optical components. The moving boundary can then be recorded at appropriate time intervals on photographic film, on chart paper, or as digital output fed directly into a PC. Measurement of the rate of the movement of the boundary (per unit centrifugal field) enables evaluation of the sedimentation coefficient. (For an introduction, see van Holde, 1985; for more detail, see two recent books: Harding et al., 1992a; Schuster and Laue, 1994). There are three principal optical systems which can be employed: (i) absorption optics (in the range 200–700 nm), (ii) "Schlieren" refractive index gradient optics, and (iii) Rayleigh interference optics. The simplest system is the absorption system and the only commercially available analytical ultracentrifuge currently available is based around this (we will describe the operation of this here). Use of the other optical systems requires more specialized knowledge and the interested protein chemist needs really to consult an expert.

Use of an Analytical Ultracentrifuge with a Scanning Absorption Optics Detection System and On-line Data Capture to a PC

Double sector cells are used with the solution (0.2–0.4 ml) in one sector and the reference buffer or solvent in the other, the latter filled to a slightly higher level to avoid complications caused by the signal coming from the solvent meniscus. The scanning system subtracts the absorption of the reference buffer from the solution. Electronic multiplexing allows multiple hole rotors to be used so that samples can be run several at a time.

In Figure 3a, examples of sedimenting boundaries recorded using absorption optics are shown. Fig 3a (top) is for a highly purified preparation of an enzyme (methylmalonyl mutase). Fig. 3a (lower) is for a heterogeneous preparation of a DNA-binding protein (Pf1) with a macromolecular component and a fast moving aggregate; the virtue of the technique for assaying the purity of a preparation (number and asymmetry of boundary/ boundaries for a given scan) can be directly seen. Although commercial software is available for identifying the center of the sedimenting boundary (strictly the "second moment" of the boundary is more appropriate; practically there is no real difference), in practice the simplest way is (i) to plot out the boundaries (recorded at appropriate time intervals) using a high resolution printer or plotter and to graphically draw a line through the user-identified boundary centers and then (ii) use a graphics tablet to recapture the central boundary positions as a function of radial position. Computer routines such as XLA-VEL (Cölfen and Harding, unpublished) yield the sedimentation coefficient and a correction to the loading concentration for average radial dilution during the

run (caused by the sector shape of the cell channels). Other routines are available based on the total concentration distribution such as SVEDBERG (Philo, 1994) and measurement of the apparent distribution of sedimentation coefficients, g(s) such as DCDT (Stafford, 1992). The sedimentation coefficient, s, equals rate of movement of boundary/ unit centrifugal field, that is

$$s = (dr/dt)/\omega^2 r \tag{7}$$

where r is the radial position of the boundary at time t and ω is the angular velocity in rads/sec (= rpm $\times$ $2\pi/60$). For a small globular protein of sedimentation coefficient of about 2 Svedbergs (S, where 1 S = 10^{-13}sec), a rotor speed of 50000 rpm will give a measurable set of optical records after some hours. For larger protein systems (e.g. 12S globulins or 30S ribosomes) speeds of <30000 rpm are appropriate. The standard temperature at which sedimentation coefficients are quoted is now 20.0 °C (sometimes 25.0 °C). If the protein is thermally unstable, temperatures down to around 4°C can be used without difficulty. The concentration used depends on the extinction coefficient of the protein. The lower the protein concentration the better, since it minimizes problems of nonideality. For proteins of average extinction at 280 nm (≈500 ml g^{-1} cm^{-1}), concentrations as low as 0.2 mg/ml are possible with the standard 12 mm optical path length cells. This limit can be pushed even lower if the peptide bond wavelength is used (210–230 nm) and the buffer is transparent. For absorbances greater than 3, shorter path length cells need to be employed instead (minimum ≈ 3 mm: below this, cell window problems become significant), or "off-maximum" wavelengths used (with caution), or more desirably, a different optical system used (interference or Schlieren). For each concentration used, the sedimentation coefficient, s, is corrected to standard conditions of buffer/solvent density and viscosity (water at 20.0 °C):

$$s_{20,w} = s \cdot \{\eta/\eta_{20,w}\} \cdot \{(1-\bar{v}\rho_{20,w})/(1-\bar{v}\rho)\} \tag{8}$$

where ρ is the density of the solvent. Knowledge of a parameter known as the "partial specific volume", $\bar{v}$ (essentially the reciprocal of the anhydrous macromolecular density), is needed; this can usually be obtained for proteins from amino acid composition data (Perkins, 1986) or measured with a precision density meter (Kratky et al., 1973). Typically, $\bar{v} \approx 0.73$ml/g for proteins.

Extrapolation to Zero Concentration

As with $D_{20,w}$, $s_{20,w}$ is plotted versus c (the latter corrected for radial dilution) and extrapolated (usually linearly) to zero concentration (Figure 3b) to give a parameter, $s^0_{20,w}$, which can be directly related to the frictional properties of the macromolecule (the so-called "frictional ratio") and from which size and shape information can be inferred. (If the protein is very asymmetric or solvated, plotting $1/s_{20,w}$ versus c generally gives a more useful extrapolation). The downward slope of a plot of $s_{20,w}$

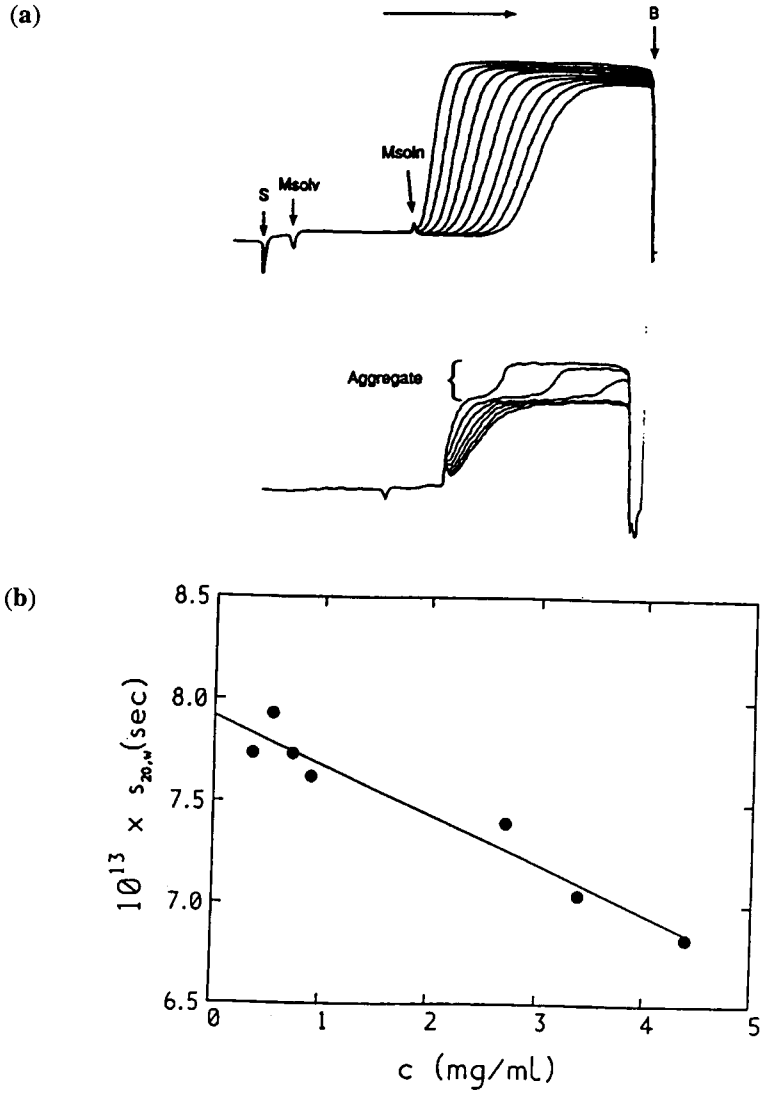

Figure 3. Sedimentation velocity in the analytical ultracentrifuge using scanning absorption optics. (**a**) Sedimentation "diagrams", Methylmalonyl mutase, c≈0.7 mg/ml. Monochromator wavelength = 295 nm; scan interval 9 min, rotor speed 44000 rev/min, temperature = 20.0 °C, measured s_{20} = (7.14±0.04)S. (**b**) Sedimentation diagrams, Gene 5 DNA binding protein, c≈ 0.7 mg/ml. Monochromator wavelength = 278 nm; scan interval 8 min, rotor speed 40000 rev/min, temperature = 20.0 °C, $s^0_{20,w}$ = (35.5±1.4)S (faster boundary) and (2.6±0.1)S (slower boundary). (**c**) Sedimentation coefficient $s_{20,w}$ versus concentration plot for an antibody (rat IgE). $s^0_{20,w}$ = (7.92±0.06)S

versus concentration is a result of nonideality behavior and is characterized by the "Gralen" parameter k_s in the equation

$$s_{20,w} = s^0_{20,w}\,(1 - k_s c) \tag{9}$$

k_s, which depends on nonideality effects of the system, will depend on the size, shape, and charge on the protein. If the solvent used is of a sufficient ionic strength, I, then these charge effects can be suppressed.

The molar mass, M, can then be found by combination of $s^0_{20,w}$ with $D^0_{20,w}$ using the Svedberg equation (Svedberg and Pedersen, 1940):

$$M = \{s^0_{20,w}/D^0_{20,w}\}\cdot\{RT/(1-\bar{v}\rho_{20,w})\} \tag{10}$$

An accurate estimate for $\bar{v}$ as described above is normally required, because, for proteins, errors are triplified; for example, an error of ±1% in $\bar{v}$ results in an error of ±3% in M. This means that care has to be made if the protein is glycosylated since the $\bar{v}$ of carbohydrate is typically ≈ 0.6 ml/g.

For a heterogeneous system, $s^0_{20,w}$ will be a weight average and $D^0_{20,w}$ will be a z-average; the M calculated will also be a weight average (Pusey, 1974) thus distinguishing it from molar mass obtained by osmometry (see Tombs and Peacocke, 1974), which yields a number average.

A further estimate can be obtained by combining $s^0_{20,w}$ simply with k_s (Rowe, 1977)

$$M = (6\pi\eta_{20,w}s^0_{20,w})^{1.5}\,\{(3\bar{v})/4\pi).[(k_s/2\bar{v}) - (v_s\sqrt{\bar{v}})]\}^{0.5} \tag{11}$$

where v_s is a specific volume allowing for hydration of the protein, and since the ratio $(v_s/\bar{v})$ is usually small in comparison with $(k_s/2\bar{v})$, an approximate estimate normally suffices. This method has given reliable values for standard protein molecules of known molar mass (Rowe, 1977). k_s itself is a valuable parameter for shape measurement as is discussed below. The form of the concentration dependence can also be used as an assay for self-associating systems (Rowe, 1977), although sedimentation equilibrium methods (see below) are usually superior.

Sedimentation Equilibrium

The "sedimentation–diffusion" method (Equation 10) for giving molar mass, although absolute, is rather inconvenient in requiring two sets of measurements. A simpler method is to use the analytical ultracentrifuge by itself with the technique known as sedimentation equilibrium, and it is probably the method of choice for molar mass determination of intact protein assemblies and particularly for the investigation of interacting systems of proteins (Schachman, 1989). The same instrument and optical system(s) for sedimentation velocity are used, the principal differences being (i) the much lower rotor speeds employed, (ii) the longer run times, and (iii) the shorter solution (and buffer) columns in the ultracentrifuge cell–hence the smaller amount of material required.

Sedimentation equilibrium, unlike sedimentation velocity, gel filtration, and dynamic light scattering, is not a transport method. In a sedimentation equilibrium experiment, the rotor speed is chosen to be low enough so that the forces of sedimentation and diffusion on the macromolecular solute become comparable allowing an equilibrium distribution of solute to be attained. This equilibrium can be established after a period of 2 to 96 hours depending on the macromolecule, the solvent, and the run conditions. Since there is no net transport of solute at equilibrium, the recording and analysis of the final equilibrium distribution (Figure 4) will give an absolute estimate for the molar mass and associated parameters since frictional (i.e., shape) effects are not involved.

In this description, we again, for simplicity, refer only to the absorption system, because of its simplicity and availability, for recording the distribution of solute in the ultracentrifuge cell—this time an equilibrium distribution. The most accurate method is in fact the interference system, but this requires considerable more expertise to operate correctly (the reader is referred to references Van Holde, 1985; Harding et al., 1992a; Schuster and Laue, 1994.) The concentration and volume requirements for the macromolecular solute depend more critically, compared to sedimentation velocity, on the extinction coefficient of the protein. Like sedimentation velocity and dynamic light scattering, the lower the protein concentration the better, since it minimizes problems of thermodynamic nonideality. At higher concentrations (necessary if possible associative phenomena are being investigated - such as at the concentrations used for NMR measurements), the limitation is the Lambert Beer law. The proportionality $c \propto$ absorbance (A) fails above absorbances of about 1.4 to 1.5. For concentrations of 1 mg/ml and above, shorter path length cells need to be employed or an ultracentrifuge with Schlieren optics employed. Volume requirements are lower than for sedimentation velocity: generally 0.1 to 0.2 ml. The longer the column, the greater the precision and the more information that can be extracted. The shorter the column, the quicker equilibrium can be reached. Experimental times can be long. For molecules of $M<10000$, <24 h are required; large, slower diffusing molecules take 48 to 72 h, although for the latter, time to equilibrium can be decreased by initial "overspeeding", that is, running at higher speed for a few hours before setting to the final equilibrium speed. It may, in some applications, be desirable to use shorter columns (as low as 0.5 mm); although the accuracy of the molar masses will be lower, this "short column" method offers the advantage of fast equilibrium (few hours) (Correia and Yphantis, 1992), which may be important if many samples need to be run and/or the macromolecule is relatively stable. As with sedimentation velocity, a temperature of 4 °C can be used without difficulty.

If scanning absorption optics are used, equilibrium patterns such as in Figure 4 can be read directly into an attached PC. As with sedimentation velocity, cells can be run multiply in multihole rotors and electronically multiplexed. In addition, special multichannel cells containing three solution/solvent pairs can be used, and this is illustrated in Figure 4. So for a four-hole ultracentrifuge rotor (with 1 hole

needed for the counterpoise with reference slits for calibrating radial positions in the cell), nine solutions can be run simultaneously.

Before interpretation in terms of molar mass, a baseline is normally required. After the final equilibrium pattern has been recorded (equilibrium checked by comparing scans separated by a few hours), the rotor is run for a short time at a higher speed (up to 60000 rev/min or the upper limit for a particular centerpiece) to deplete the solution—or at least the meniscus region—of solute: the residual absorbance gives the baseline correction (absorbance of nonmacromolecular species). This is not so easy with small proteins whose equilibrium speed will be quite

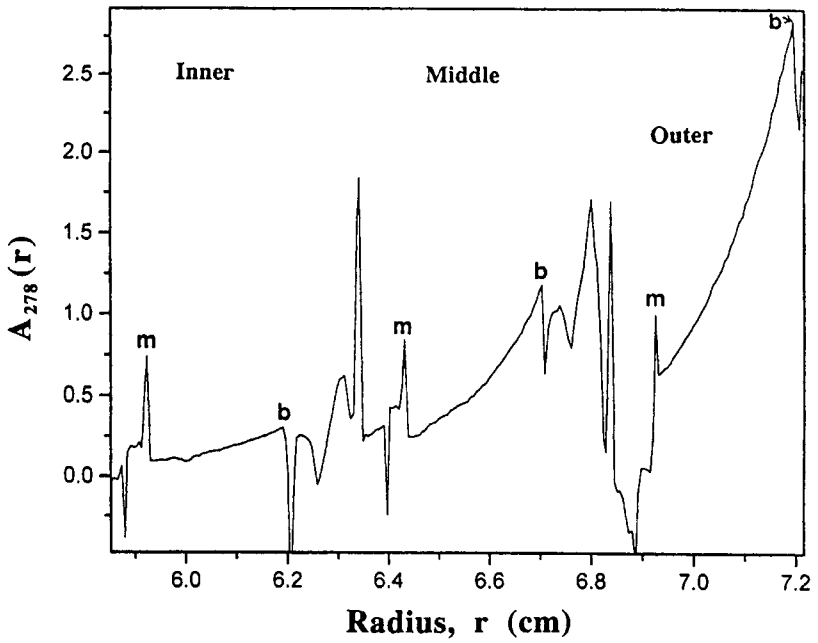

Figure 4. Sedimentation equilibrium profiles for β-lactoglobulin B. Absorption optics, wavelength = 280 nm. Rotor speed = 15000 rev/min, temperature = 20.0 °C. A multichannel cell (12 mm optical path length) was used allowing three solution/solvent pairs with ≈0.12 ml in solvent channels, ≈0.10 ml in solution channels. Inner profile: loading concentration c = 0.1 mg/ml; middle:0.2 mg/ml; outer = 0.3 mg/ml. Because of restrictions from the Lambert-Beer law, with the outer channel, only absorbances <1.5 could be used. This difficulty could be offset by using a higher wavelength. With the inner channel, the signal could be increased by using far-uv optics (210–230 nm).

high anyway: careful dialysis of solution versus the reference solvent before the run (and use of the dialysate as reference) may be necessary.

The average slope of a plot of ln A versus r^2, the square of the radial distance from the center of the rotor, will yield the molar mass:

$$M = (d\ln A/dr^2) \times 2RT/(1 - \bar{v}\rho)\,\omega^2 \qquad (12)$$

At finite concentrations, this will be an apparent molar mass (because of the effects of thermodynamic nonideality; see below), but for macromolecular systems of $M \leq$ 100,000 g/mol in aqueous solvents of reasonable ionic strength (0.05 M and above), these effects are small at loading concentrations of 0.5 mg/ml and less: in these cases, it is reasonable to assume $M \approx M_{w,app}$.

If the protein solution is heterogeneous (containing interacting or noninteracting species of different molar mass), then the plot of ln A versus r^2 will be curved upwards. This situation occurs with self-associating systems and heavily glycosylated protein systems such as mucus glycoproteins. In this case, the data can be treated in one of two ways: (i) an average slope is obtained. This yields, as with equation 12, the weight average molar mass, M_w. For strongly curving systems or for systems where the cell base is not clearly defined, a procedure that uses a function known as M^* (Creeth and Harding, 1982; Harding et al., 1992b) is useful for this purpose; (ii) local slopes using a sliding strip procedure (Teller, 1973) along the ln A versus r^2 curve can be obtained to give what is called apparent "point" weight average molar masses, $M_{w,app}(r)$, as function of either radial position (or the equivalent local concentration or absorbance). This procedure is particularly useful for the investigation of self-association phenomena and other types of heterogeneity and also provides a method for extracting the z-average molar mass:

$$M_{z,app} = \{M_w(r_b)\cdot A(r_b) - M_w(r_a)\cdot A(r_a)\}/[A(r_b) - A(r_a)] \qquad (13)$$

where (r_a, r_b) are the radial positions of the solution meniscus and cell base respectively, and $M_{z,app} \rightarrow M_z$ as the concentration (in absorbance units, A) $\rightarrow$ 0.

The ratio M_z/M_w can be used as an index of the heterogeneity of the sample, and, for noninteracting systems, is a measure of the inherent polydispersity of a system; this is particularly relevant to the study of heavily glycosylated systems, for example.

If the system is self-associating or involved in "heterologous" association (i.e., complex formation phenomena), then either the A(r) versus r plot (Figure 5a), the $M_{w,app}(r)$ versus A(r) plot, or a plot of $M_{w,app}$ versus c for different loading concentrations, c, can be used to assay for the stoichiometry and strength of an interaction. There are several commercial software packages available: see Cölfen et al. (1997). Assays are also available for distinguishing between a self-association from noninteracting mixtures (Roark and Yphantis, 1969).

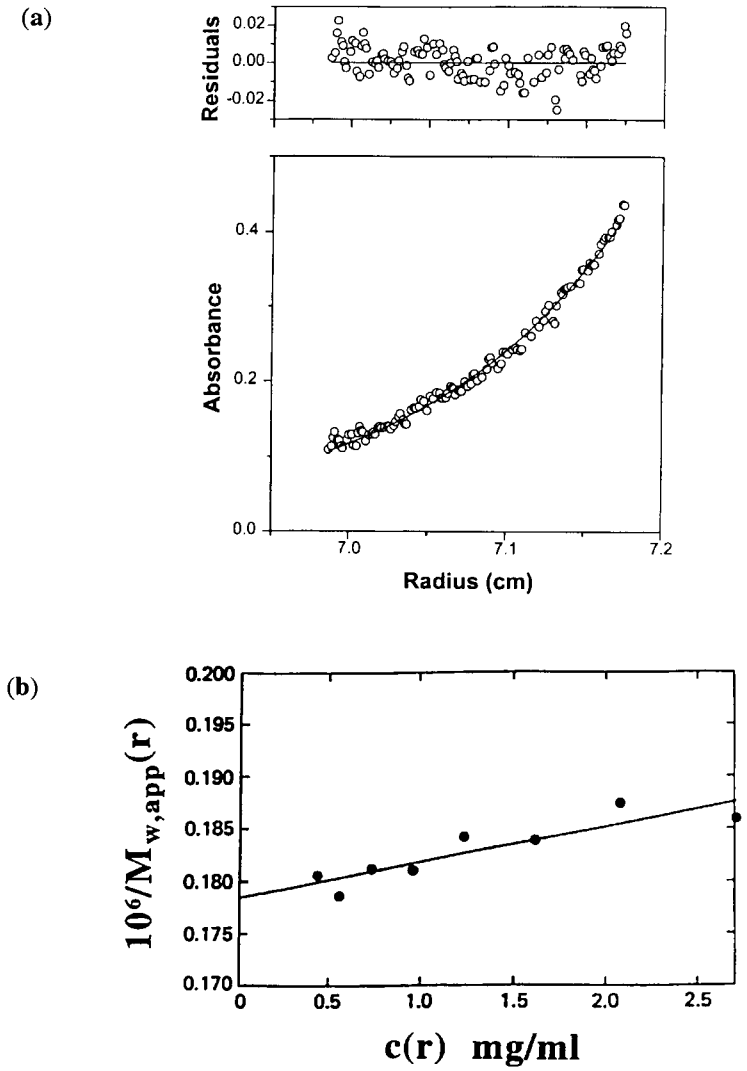

Figure 5. Analysis of sedimentation equilibrium data self-association analysis. (**a**) Self-association: Absorbance A(r) versus radial displacement (r) data for protein disulphide isomerase (PDI). Rotor speed = 12000 rpm, temperature = 4 °C, loading concentration, c = 0.4 mg/ml. Line fitted is for a reversible ideal dimerization, dissociation constant, $K_d \approx 180$ μM (from Darby et al., 1997). (**b**) Thermodynamic nonideality: Plot of the reciprocal point (apparent) average molar mass $M_{w,app}$ (r) as a function of radial position, r, versus concentration, c(r), for turnip-yellow mosaic virus (TYMV) . M_w (from extrapolation to zero concentration) = (5.8 ± 0.2) × 10^6 g/mol. Adapted from Harding and Johnson (1985).

For larger macromolecules ($M \geq 100000$) such as protein assemblies and heavily glycosylated systems and/or for more concentrated solutions, nonideality (through macromolecular exclusion and any unsuppresed charge effects) may become significant, and this will tend to cause downward curvature in the ln A versus r^2 plots: this can often obscure heterogeneity phenomena and the two effects (nonideality and heterogeneity can occasionally cancel to give a linear plot that can be misleading, a problem that can be avoided by running at more than one loading concentration). If the solution is not significantly heterogeneous, then a simple extrapolation from a single experiment of point (apparent) molar mass to zero concentration (absorbance) can be made in order to give the infinite dilution "ideal" value (in general, reciprocals are usually plotted; see Figure 5b). Alternatively, several sedimentation equilibrium experiments performed at different loading concentrations, c, and extrapolation of "whole cell" molar masses $M_{w,app}$ to zero concentration are necessary.

Insofar as modern computing packages are concerned, software currently available from the commercial manufacturer tends to require an assumed model prior to the analysis (ideal monomer, self-association, nonideal self-association, etc.). We find a general package, of use that does not require assumed models. This is MSTAR (Harding et al., 1992b), now available for PC (Cölfen and Harding, 1997). This program evaluates $M_{w,app}$ (using the M^* function), $M_{w,app}(r)$ versus r or A, and also $M_{z,app}(r)$, if the data is of sufficiently high quality. After these model independent analyses have been performed, resort can *then* be made to the more specialized packages (self-association, polydispersity, etc.).

SHAPE MEASUREMENT

Hydrodynamic methods provide a relatively quick method to acquire average or "gross" conformation information about proteins and protein assemblies, and in some cases to give rather detailed representations, as for example for T-even bacteriophages and antibodies. Limited flexibility information is also possible. Although such information may seem to be "low-resolution" compared to the information possible from the powerful structural probes of x-ray crystallography and high-resolution NMR, it should be borne in mind that the latter are sometimes not applicable for the following reasons: (i) high enough aggregation-free concentrations necessary for high-resolution NMR may not be attainable for a given protein system or assembly; (ii) the protein or protein assembly may not be crystallizable, or molecular flexibility effects may obscure attempts to interpret electron density maps: the latter is the reason why crystallographers have had considerable difficulty in evaluating the structure of intact, immunologically active antibody molecules.

In both these cases, hydrodynamic methods are particularly valuable (i) to monitor possible associative behavior at higher concentration (using any of the techniques above, particularly sedimentation velocity and equilibrium) and (ii) to

provide conformation information of the protein or protein assembly in in-vivo solution conditions; this can be either in terms of an overall shape or in terms of refinement of a crystal structure of a protein or electron microscopic structure of a protein assembly (arrangement of subunits). A good example is the case of antibodies with a useful early attempt made by Gregory and colleagues (1987).

Modelling Strategies: Spheres, Ellipsoids, Beads, and Bends

Hydrodynamic representation of protein shape is in terms of models that progress in sophistication from a sphere to bead models (Figure 6). The simplest is the equivalent hydrodynamic (or "Stokes") sphere, of radius r_H (cf. equation 6). The next step toward better representation is the ellipsoid of revolution, an ellipsoid with two equal axes of which there are two: the prolate ellipsoid (cigar shape) with two equal minor axes and the oblate ellipsoid (discoid) with two equal major axes, both characterized by the axial ratio a/b with the semiaxes a≥b. In the limit of a>>b, the prolate becomes a rod and the oblate a disc. The next step in sophistication is the general triaxial ellipsoid of semiaxes $a \geq b \geq c$ and axial ratios {a/b, b/c}, which in the limits go to spheres {a/b = 1; b/c = 1}, oblate ellipsoids {a/b=1}, and prolate ellipsoids {b/c=1}, the latter two going to discs and rods respectively. Another extreme of the general ellipsoid is the tape (a >> b >> c). The final degree of sophistication is the bead model: many macromolecules such as antibodies and multisubunit proteins are difficult to represent by symmetric shapes like ellipsoids.

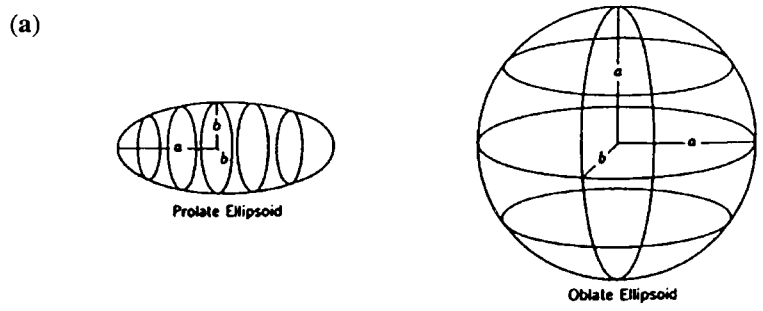

Figure 6. Hydrodynamic models for conformation. (**a**) Ellipsoids of revolution (adapted from Tanford, 1961). (**b**) General triaxial ellipsoids. (**c**) Bead models. (*i*) T-even bacteriophage in slow(s) and fast(f) forms ($s^0_{20,w} \approx$ 710S and 1020S, respectively). Modelled on sedimentation and diffusion coefficient data. From Garcia de la Torre (1989). (*ii*) C1 complex from the complement system. Modelled on sedimentation coefficient and R_g data. From Perkins (1989). (*iii*) Cyclic AMP receptor associated with 80-bp DNA. Only maximum bending of the DNA reproduces the measured rotational diffusion decay constant (from electric dichroism decay). From Pörschke and Antosiewicz (1989).

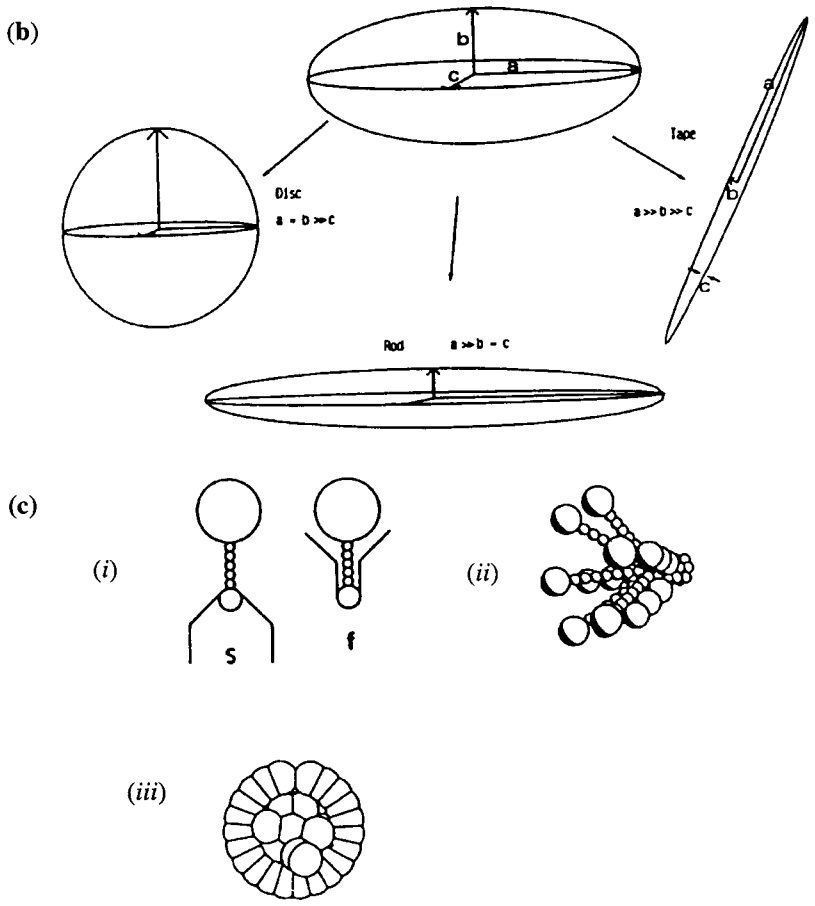

Figure 6. Continued

Bead modelling (arrays of touching or overlapping spheres) allows very sophisticated shapes to be represented. A successful variant of this is bead-shell modelling, where the surface of the macromolecule is represented by beads. Filling strategies, however, such as those based on crystallographic coordinates, have sadly been shown (Carrasco, 1998) to be unreliable.

As the degree of sophistication increases, the *uniqueness problem* also increases. What this means is that a model may be consistent with a particular measured hydrodynamic parameter such as a sedimentation coefficient $s^0_{20,w}$ or a radius of gyration R_g (from solution x-ray scattering or light scattering; see, for example, Van Holde, 1985) but so may other models. For example, a value for the sedimentation coefficient can correspond to *one* equivalent sphere, *two* ellipsoids of revolution, a *line solution* of triaxial ellipsoids, and almost an *infinity* of bead models. There is

a further problem from ellipsoids upward: hydration or the degree of buffer/solvent associated with (chemically bound or physically entrapped) by the protein - which also contributes to $s^0_{20,w}$ among other things and has to be either measured separately, assumed, or eliminated by combination of measurements. As the degree of sophistication in the model increases, there is a greater need for independent measurements (two for ellipsoids of revolution, three for triaxial ellipsoids to give a "unique" answer). Bead modelling, normally performed with at least two hydrodynamic measurements (popularly $s^0_{20,w}$ or $D^0_{20,w}$ and R_g , although rotational probes have been used; Antosiewicz and Pörschke, 1989; Pörschke and Antosiewicz, 1989) is best used to refine a structure from crystallography or to select between certain plausible structures. A further refinement to bead modelling is in the modelling of molecular flexibility, the bending or "segmental flexibility" in the molecules. Details of this and its application to flexibility phenomena in myosin can be found in Garcia de la Torre (1989), Garcia de la Torre and Bloomfield (1977); Garcia de la Torre (1992), and Garcia de la Torre (1994). Finally, bead and bead-shell strategies have been developed based on shape alone, without the ambiguities caused by size (Garcia de la Torre et al., 1997).

Intrinsic Viscosity

The simplest hydrodynamic conformation measurement is the intrinsic viscosity. The classical reference on the theory and practice of protein viscometry is an article by J.T. Yang (1961). A more recent effort has been written by the present author (Harding, 1997). The viscosity of an aqueous solvent will be increased by the addition of a macromolecular solute to an extent depending on (i) the concentration, (ii) the size (including the degree of hydration), and (iii) the shape. Increased concentration, size, and shape all increase the viscosity of a solution.

Viscosity measurements on proteins in dilute solution are normally performed in a capillary (or "Ostwald") viscometer with the flow time under gravity (between two reference points) of the solution (t) compared to that of the solvent (t_o), although differential microviscometers based on a pressure imbalance principle appear highly promising (Haney, 1985).

With conventional capillary viscometers, pumping of liquid and timing is now usually done automatically, employing photodetectors (using, for example, a Schött-Geräte (Hofheim, Germany) system) and because viscosity is a sensitive function of temperature, a water bath is required with the temperature controlled and measured to within ± 0.005 °C. From the flow times (averaged over consistent measurements), the relative viscosity is η_r obtained from

$$\eta_r = (t/t_o)\cdot(\rho/\rho_o) \qquad (14)$$

with (ρ/ρ_o) the ratio of the solution to solvent density. This can be measured separately for each concentration using a precision density meter (Kratky et al., 1973; Rowe, 1978), but more conveniently this can be avoided if we use a kinematic

relative viscosity $\eta'_r = (t/t_o)$ and use a correction factor in the data analysis (see below) (Tanford, 1955).

A (kinematic) reduced specific viscosity is then defined

$$\eta'_{red} = (\eta'_r - 1)/c \tag{15}$$

so if c is in g/ml, η'_{red} is in ml/g. To eliminate nonideality effects, η'_{red} is measured at a series of concentrations and extrapolated to zero concentration to yield the (kinematic) intrinsic viscosity $[\eta']$ which can then be corrected for density to give the ("dynamic") intrinsic viscosity $[\eta]$.

$$[\eta] = \{(1 - \bar{v}\rho_o)/\rho_o\} + [\eta'] \tag{16}$$

The shape parameter, known as the "viscosity increment" ν (see for example, Tanford, 1961; Harding, 1995) is obtained from

$$\nu = [\eta] / v_s \tag{17}$$

where v_s(ml/g), the "swollen specific volume", is the volume of the "hydrated" protein per unit mass of dry protein and is related to the partial specific volume $\bar{v}$ by $\bar{v}_s = \bar{v} + (\delta/\rho_o)$, where δ (sometimes symbol "w") is known as the "hydration", the number of grams of solvent bound per gram of dry protein. Or, in terms of protein volume, V, $v_s = VN_A/M$ where V (ml) is the (hydrated) volume of the protein and N_A is Avogadro's number. Since ν is the Einstein (1906, 1911) 2.5 value for spheres and since $V = (4/3)\pi r_H^3$ the hydrodynamic radius can be found thus providing an alternative procedure to dynamic light scattering for its measurement. ν has also been evaluated for *prolate and oblate ellipsoid* models. Although the direct formulae are complicated (Harding, 1995), simple polynomial approximations that are accurate to ±1% are available (Harding and Cölfen, 1995) and hence, provided a value for v_s (or δ) is known or assumed, the axial ratio a/b can be found. The value typically taken for δ for proteins is about 0.35 ($\equiv v_s \approx 1$), although for unconjugated proteins it can vary by about ±100%, and for heavily glycosylated proteins such as those from mucus secretions, δ can be as high as about 70 (Harding et al., 1983). (Caution has to be expressed when assigning a conformation from viscosity data alone.) For *triaxial ellipsoids*, evaluation of ν merely specifies a *line solution* of possible values of (a/b, b/c) between the extremes of prolate ellipsoid (b/c = 1) and oblate ellipsoid (a/b=1) (Figure 7). Besides an assumption over δ, a further independent hydrodynamic measurement is necessary to provide a graphical intersection with the ν-line to specify (a/b, b/c) directly.

For the case of *bead modelling*, computer programs are available such as HYDRO (Garcia de la Torre et al., 1994) or the more recent size-independent SOLPRO algorithm (Garcia de la Torre et al., 1997) for predicting ν (or $[\eta]$) for a given specified set of coordinates for the beads; this procedure can thus be used for selecting which model gives the desired $[\eta]$ (after assuming a value for δ). Because of the uniqueness problems referred to above, for bead modelling the $[\eta]$ data

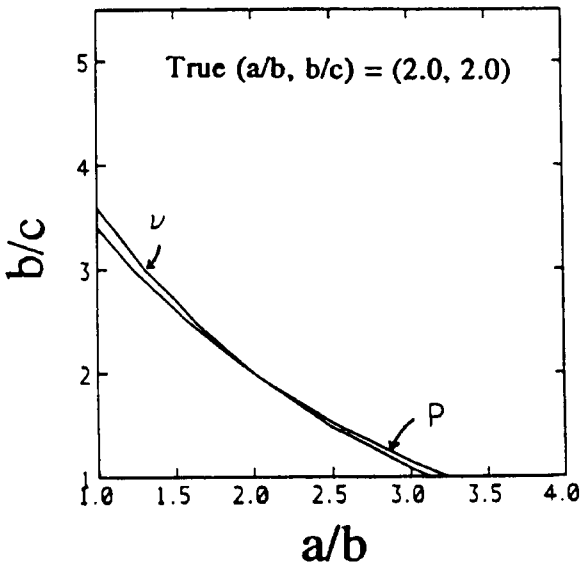

Figure 7. Plots of constant values (i.e., "line solutions") for ν and P as a function of the two triaxial ellipsoid axial ratios. Simulated data, for a hypothetical molecule of "real" {a/b, b/c} = (2.0, 2.0). Adapted from Harding and Rowe (1983). The intersection is supposed to give a unique value for (a/b; b/c), although this particular choice of shape functions gives too-shallow an intersection.

cannot be used in isolation but has to be combined with other hydrodynamic measurements (e.g., sedimentation, diffusion, x-ray scattering, rotational diffusion, etc.).

Sedimentation Velocity and Dynamic Light Scattering

The principal conformation parameter to come out of both these measurements is known as the frictional ratio (f/f_o). This is the ratio of the frictional coefficient of the protein to the frictional coefficient of a rigid spherical particle of the same anhydrous mass and volume. This can be related to either $s^0_{20,w}$ or $D^0_{20,w}$ by

$$(f/f_o) = (M(1 - \bar{\nu}\rho_0)/N_A \cdot 6\pi\eta_0 s^0_{20,w}) (4\pi N_A/3\bar{\nu}M)^{1/3} \quad (18)$$

or

$$(f/f_o) = \frac{k_B T}{6\pi\eta_0}\left(\frac{4\pi N_A}{3\bar{\nu}M}\right)^{1/3} \cdot \frac{1}{D^0_{20,w}} \quad (19)$$

(see for example, Tanford, 1961; Harding, 1995) where, η_0 is the viscosity of water at 20.0 °C. In order to get shape information from equations 18 or 19, first of all a

function P (named in recognition of F. Perrin, who worked out the theory for the frictional coefficients for ellipsoids) is defined:

$$P = (f/f_o) \cdot [(\delta/\bar{v}\rho_{20,w}) + 1]^{-1/3} \quad (20)$$

and then, similarly to viscometry, if δ is known or assumed, P can be obtained. The "Perrin function" P is analogous to the viscosity increment ν, and the axial ratio (a/b) for an ellipsoid of revolution can be found either by a rather complicated expression involving an elliptic integral or by simple polynomial expansions available for both prolate and oblate ellipsoids (Harding and Cölfen, 1995). For general triaxial ellipsoids, as with ν, there is a line solution of possible values for P (Figure 7). In principle, {a/b, b/c} can be found from the graphical intersection but as is clear from Figure 7, this is too shallow to cope with any data error. Other combinations involving these or other shape functions need to be employed.

Use of Concentration Dependence Parameters, Combined Shape Functions, and the Radius of Gyration R_g

A simple way in principle to solving the hydration problem is to combine two shape functions together in such a way that the experimental requirement for δ or v_s is eliminated to give a combined "hydration-independent" shape function. The simplest of these is known as the β-function and comes from combination of equations 17 with 18 or 19 (see, for example, Tanford, 1961; Van Holde, 1985; Harding, 1995). This function is unfortunately highly insensitive to shape and of very limited use for conformation analysis; in fact it has found more use as a quasi-constant parameter for enabling M to be calculated from $[\eta]$ and $s^0_{20,w}$ or $D^0_{20,w}$ (Yang, 1961). A more useful combination is $[\eta]$ with k_s, the concentration dependence regression parameter from sedimentation velocity measurements (cf. equation 9), provided the sedimentation measurements have been made in a buffer of sufficient ionic strength, I, to suppress charge effects. To an approximation, (Rowe, 1992; Rowe, 1977) the ratio

$$R = \{k_s/[\eta]\} \approx 2(1 + P^3)/\nu \quad (21)$$

Another is a combination of the second thermodynamic virial coefficient, B (from the concentration dependence of the apparent molar mass measurements using sedimentation equilibrium), with $[\eta]$ to define the hydration-independent shape, function Π (Harding, 1981; 1995).

$$\Pi = \{2BM/[\eta]\} - f(Z,I)/\{[\eta]M\} \quad (22)$$

where the 2nd term on the RHS [a function of molecular charge or valency (Z) and ionic strength (I)] goes to zero if the ionic strength is sufficient (normally ≥ 0.3M). As with ν and P above, both R and Π are available as simple polynomial expansions in terms of axial ratio a/b for ellipsoids of revolution (Harding and Cölfen, 1995). They are also available as line solutions for {a/b, b/c} for triaxial ellipsoids and of

course have the advantage over ν and P of not requiring an assumption concerning hydration for their measurement. Unfortunately, plotting R with Π gives an equally poor intersection as that shown in Figure 7. A better combination is Π with the radius of gyration shape function G defined by (Harding, 1987)

$$G = \{(4\pi N_A)/(3vM\}^{2/3} \cdot R_g^2 \tag{23}$$

R_g derives from a light scattering (or x-ray or neutron scattering) measurement, and if the surface (aq.) solvent on the protein is to a good approximation indistinguishable from surrounding solvent, and if the protein is not internally swollen through hydration, the specific volume term in equation 23 refers to the anhydrous protein ($v \approx \bar{v}$) and no assumed value for the hydration is required. G also has a line solution for triaxial ellipsoids, but graphical combination of G with Π does give a reasonable intersection and has been used to investigate the overall conformation of myosin in solution (Harding, 1987).

Insofar as bead modelling is concerned, R_g (i.e., G) from x-ray and neutron scattering and $s^0_{20,w}$ (or P) have been used *within the limitations referred to above* with the earlier modelling program TRV (Garcia de la Torre, 1989) to distinguish plausible conformations for antibody models (Gregory et al., 1987) and has been used to show these molecules are clearly not coplanar as sometimes rather misleadingly depicted in textbooks. R_g with $s^0_{20,w}$ has been used to select appropriate models for the complement system (Perkins, 1989) (see Figure 6) and a combination of $D^0_{20,w}$ and $s^0_{20,w}$ used to model the self-assembly of T-even bacteriophages (Garcia de la Torre, 1989; Garcia de la Torre and Bloomfield, 1977). R_g combined with $[\eta]$ and electrooptic data has been used to model the flexibility of regions of myosin between the S2 head and low meromyosin (LMM) in terms of bending energies (Iniesta et al., 1989; Garcia de la Torre, 1989).

Measurement and Use of Rotational Hydrodynamic Shape Functions: Fluorescence Depolarization Decay

A protein in solution will be subject to Brownian rotational forces. The ease or rate at which a protein rotates will depend on its size, shape, and hydration—in common with the three factors that also determine rate of translational diffusion. Therefore, if the size and hydration are known (or can be eliminated by combination with another measurement), then measurement of the rotational diffusion property can be used as another probe to measure shape. Although these measurements tend to be more difficult, the incentive is that the shape functions so derived are more sensitive functions of shape. The principal methods have been flourescence depolarization, electro-optics and, more recently, nuclear magnetic resonance (Garcia de la Torre et al., 1998).

The most popular rotational diffusion probe is fluorescence depolarization (Weber, 1952; Van Holde, 1985). With the fluorescence depolarization method, fluorescent light emanating from a stimulated (by polarized light at the appropriate

wavelength) protein with a suitable fluorescent chromophore (either intrinsic—tryptophan, or synthetically attached) will be plane polarized. As the proteins rotate under rotational Brownian forces, the degree of polarization will decay at a rate dependent on the speed of rotation of the molecules. Detectors fitted with polarizers are used to measure the intensity of light parallel ($I_\perp$) and perpendicular ($I_\parallel$) to the incident pulse and the anisotropy measured

$$A = (I_\perp - I_\parallel)/(I_\perp + 2I_\parallel) \tag{24}$$

In the "steady-state method", the protein solution is continuously irradiated and by making measurements of A in solutions at a variety of temperatures and viscosities (usually with the addition of glycerol) and with knowledge of the fluorescent lifetime of the chromophore, the harmonic mean relaxation time τ_h (units: sec.) can be measured from extrapolating a plot of $1/A$ versus T/η_o to $T/\eta_o = 0$ (Van Holde, 1985; Weber, 1952) η_o is the solvent viscosity at temperature T. As with other hydrodynamic parameters, in principle, τ_h needs to be extrapolated to zero concentration to eliminate any possible contributions from nonideality effects.

To obtain shape information from τ_h, a ratio $\{\tau_h/\tau_o\}$ is defined (by analogy with the Perrin P function) where

$$\{\tau_h/\tau_o\} = (kT\tau_h)/(\eta_o V) \tag{25}$$

and where the volume of the protein $V = v_s M/N_A$.

To remove the requirement of knowledge of v_s (i.e., hydration), $\{\tau_h/\tau_o\}$ is combined with $[\eta]$ to produce the hydration-independent parameter Λ (Harding, 1980, 1995; Harding and Rowe, 1982a).

$$\Lambda = \nu/\{\tau_h/\tau_o\} = (\eta_o[\eta]M)/(N_A kT\tau_h) \tag{26}$$

As with the other shape functions referred to above, simple polynomial equations are available that relate Λ to the axial ratio of ellipsoids of revolution, and an example of its application to the globular protein neurophysin can be found in Rholam and Nicholas (1981). It is also available for triaxial ellipsoids, and a graphical combination of Λ with R can be used to obtain {a/b, b/c} uniquely (Harding and Rowe, 1982b). Indeed, this method has been used to confirm measurements previously made using the ellipsoid of revolution model (Rholam and Nicolas, 1981) that the dimerization of neurophysin clearly occurs through a side-by-side as opposed to an end-to-end process (Figure 8). These latter references also illustrate respectively the extraction of $[\eta]$, k_s, and τ_h (and hence R and Λ) for a dimerizing system.

Some words of caution: although fluorescence depolarization, along with other rotational diffusion techniques, are particularly sensitive probes for conformation, it should be stressed that particularly for synthetically attached fluorescent chromophores, it must be established that there is no free rotation of the fluorescent chromophore with respect to the rest of the molecule; also for proteins containing more than one domain, segmental flexibility can obscure the shape measurement

However, a significant recent advance has been the design of an instrument with adequate shielding against such affects (Pörschke and Obst, 1991) to permit the use of solvents at physiological ionic strengths. The application of electric birefringence methods to triaxial ellipsoid modelling can be found in Harding and Rowe (1983) and to bead modelling in Pörschke and Antosiewicz (1989). Finally, nmr as a route for obtaining time-resolved rotational relaxation time appears highly promising (Garcia de la Torre et al., 1998).

Some Computer Programs for Conformational Analysis

For ellipsoid modelling, the ELLIPS series of program for the PC (BASIC and FORTRAN) have been developed (Harding and Cölfen, 1995; Harding et al., 1997). ELLIPS1 evaluates the axial ratio a/b for prolate and oblate ellipsoids for a user-specified value for a hydrodynamic parameter and is based on polynomial approximations to the full hydrodynamic equations: accuracy of this approximation is normally well within the precision of the measurement. ELLIPS2 uses the full hydrodynamic equations for general triaxial ellipsoids to specify the set of hydrodynamic parameters for any given value of the axial ratios {a/b, b/c}. ELLIPS3 and ELLIPS4 do the reverse procedure using a variety of graphical combinations of hydration-independent triaxial shape functions (cf. Figures 3 and 4). Elsewhere, the routine SOLPRO (Garcia de la Torre et al., 1997, 1998) is particularly useful for the application of bead models.

REFERENCES

Ackers, G. (1975). Molecular sieve methods of analysis. In: *The Proteins*, Third ed. (Neurath, H. and Hill, R.L., Eds.), p.1. Academic Press, New York.

Andrews, P. (1965). Estimation of molecular weights of proteins by Sephadex gel filtration. Biochem. J. 91, 22.

Antonsiewicz, J. and Pörschke, D. (1989). An unusual electrooptical effect observed for DNA fragments and its apparent relation to a permanent electric moment associated with bent DNA. Biophys. Chem. 33, 19.

Arner, E.C. and Kirkland, J.J. (1992). In: *Analytical Ultracentrifugation in Biochemistry and Polymer Science*. (Harding, S.E., Rowe, A.J., and Horton, J.C., Eds.), p. 209. Royal Society of Chemistry, Cambridge, England.

Barth, H.G. (1980). A practical approach to steric exclusion chromatography of water-soluble polymers. J. Chromatog. Sci. 18, 409.

Brown , W. (ed) (1993). *Dynamic Light Scattering. The Method and Some Applications.* Oxford University Press, Oxford.

Burchard, W. (1992). Static and dynamic light scattering approaches to structure determination of biopolymers. In: *Laser Light Scattering in Biochemistry* (Harding, S.E., Sattelle, D.B., and Bloomfield, V.A., Eds.), p. 3–22. Royal Society of Chemistry, Cambridge, England.

Claes, P., Dunford, M., Kennedy, A., and Vardy, P. (1992). An on-line dynamic light-scattering instrument for macromolecular characterization. In: *Laser Light Scattering in Biochemistry.* (Harding, S.E., Sattelle, D.B., and Bloomfield, V.A., Eds.), p. 66–76. Royal Society of Chemistry, Cambridge, England.

Cölfen, H. and Harding, S.E. (1997). MSTARA and MSTARI: Interactive PC algorithms for simple, model-independent evaluation of sedimentation equilibrium data. Eur. Biophys. J. 25, 333–346.

Cölfen, H., Harding, S.E., Wilson, E.K., Scrutton, N.S., and Winzor, D.J. (1997). Low temperature solution behaviour of methylophilus methylotrophus electron-transferring flavoprotein: A study by analytical ultracentrifugation. Eur. Biophys. J. 25, 411–416.

Correia, J.J. and Yphantis, D.A. (1992). Equilibrium sedimentation in short solution columns. In: *Analytical Ultracentrifugation in Biochemistry and Polymer Science*. (Harding, S.E., Rowe, A.J., and Horton, J.C., Eds.), p. 231–252. Royal Society of Chemistry, Cambridge, England.

Creeth, J.M. and Harding, S.E. (1982). Some observations on a new type of point average molecular weight. J. Biochem. Biophys. Meth. 7, 25–34.

Darby, N., Harding, S.E., and Creighton, T.E. (1997). (In Press.)

Dubin, P.L. and Principi, J.M. (1989). No previously suggested dimensional parameter controls peak migration in size exclusion chromatography. Div. Polym. Chem., Am. Chem. Soc. Preprints, 30, 400–401.

Einstein, A. (1906). Ann. Physik. 19, 289–305; and corrigenda (1911) 34, 591–592.

Garcia de la Torre, J. (1989). Hydrodynamic properties of macromolecular assemblies. In: *Dynamic Properties of Biomolecular Assemblies*. (Harding, S.E. and Rowe, A.J., Eds.), pp. 3–31, Royal Society of Chemistry, Cambridge, England.

Garcia de la Torre, J. (1992). Sedimentation coefficients of complex biological particles. In: *Analytical Ultracentrifugation in Biochemistry and Polymer Science*. (Harding, S.E., Rowe, A.J., and Horton, J.C., Eds.), p. 333–345. Royal Sociey of Chemistry, Cambridge, London.

Garcia de la Torre, J. (1994). Hydrodynamics of segmentally flexible macromolecules. *Eur. Biophys. J.* 23, 307–322.

Garcia de la Torre, J., and Bloomfield, V.A. (1977). Hydrodynamics of macromelecular complexes 3. Bacterial Viruses. Biopolymers 16, 1779–1793.

Garcia de la Torre, J., Carrasco, B., and Harding, S.E. (1997). SOLPRO: Theory and computer program for the prediction of SOLution PROperties of rigid macromolecules and bioparticles. Eur. Biophys. J. 25, 361–372.

Garcia de la Torre, J., Harding, S.E., and Carrasco, B. (1998). Calculation of NMR relaxation, covolume, and scattering-related properties of bead models using the SOLPRO computer program. Eur. Biophys. J. (in press).

Garcia de la Torre, J., Navarro, S., Lopez Martinez, M.C., Diaz, F.G., and Lopez Cascales, J.J. (1994) HYDRO: A computer program for the prediction of hydrodynamic properties of macromolecules. Biophys. J. 67, 530–531.

Gregory, L., Davis, K.G., Sheth, B., Boyd, J., Jefferis, R., Nave, C. and Burton, D.R. (1987) The solution conformations of the subclasses of human IgG deduced from sedimentation and small angle X-ray scattering studies. J. Mol. Immunol. 24, 821–830.

Han, M.K., Knutson, J.R., and Brand, L. (1989). Fluorescence studies of protein-subunit interactions. In: *Dynamic Properties of Biomolecular Assemblies*. (Harding, S.E. and Rowe, A.J., Eds.), p. 115–134. Royal Society of Chemistry, Cambridge, London.

Haney, M.A. (1985). A differential viscometer. American Laboratory 17, 41–56.

Harding, S.E. (1980). The combination of the viscosity increment with the harmonic mean rotational relaxation time for determining the conformation of biological macromolecules in solution. Biochem. J. 189, 359–361.

Harding, S.E. (1981). A compound hydrodynamic shape function derived from viscosity and molecular covolume measurements. Int. J. Biol. Macromol. 3, 340–341.

Harding, S.E. (1986). Applications of light scattering in microbiology. Biotech. Appl. Biochem. 8, 489–509.

Harding, S.E. (1987). A general method for modeling macromolecular shape in solution—a graphical (11-G) intersection procedure for triaxial ellipsoids. Biophys. J. 51, 673–680.

Harding, S.E. (1995). On the hydrodynamic analysis of macromolecular conformation. Biophys. Chem. 55, 69–93.

Harding, S.E. (1997). The intrinsic viscosity of biological macromolecules. Progress in measurement, interpretation, and application to structure in dilute solution. Prog. Biophys. Mol. Biol. 68, 207–262.

Harding, S.E. and Cölfen, H. (1995). Inversion formulae for ellipsoid of revolution macromolecular shape functions. Analyt. Biochem. 228, 131–142.

Harding, S.E. and Johnson, P. (1985). Physicochemical studies on turnip-yellow-mosaic virus. Homogeneity, relative molecular masses, hydrodynamic radii and concentration-dependence of parameters in nondissociating solvents. Biochem. J. 231, 549–555.

Harding, S.E. and Rowe, A.J. (1982a).Modeling biological macromolecules in solution. 1. The ellipsoid of revolution. Int. J. Biol. Macromol. 4, 160–164. Int. J. Biol. Macromol. 4, 160–164.

Harding, S.E. and Rowe, A.J. (1982b). Modeling biological macromolecules in solution. 3. The lambda-R intersection method for triaxial ellipsoids. Int. J. Biol. Macromol. 4, 357–361.

Harding, S.E. and Rowe, A.J. (1983). Modeling biological macromolecules in solution. 2. The general triaxial ellipsoid. Biopolymers 22, 1813–1829.

Harding, S.E. and Rowe, A.J. (1984). Modeling biological macromolecules in solution. 2. The general triaxial ellipsoid. Biopolymers 23, 843.

Harding, S.E. and Rowe, A.J., and Creeth, J.M. (1983). Further evidence for a flexible and highly expanded spheroidal model for mucus glycoproteins in solution. Biochem. J. 209, 893–896.

Harding, S.E., Rowe, A.J., and Horton, J.C. (Eds.)(1992a). Analytical ultracentrifugation in biochemistry and polymer science. Royal Society of Chemistry, Cambridge, England.

Harding, S.E., Horton, J.C., and Morgan, P.J. (1992b). MSTAR: A FORTRAN program for the model-independent molecular weight analysis of macromolecules using low speed of high speed sedimentation analysis. In: *Analytical Ultracentrifugation in Biochemistry and Polymer Science.* (Harding, S.E., Rowe, A.J., and Horton, J.C., Eds.), pp. 275–294. Royal Society of Chemistry, Cambridge, England.

Harding, S.E., Horton, J.C., and Cölfen (1997). The ELLIPS suite of macromolecular conformation algorithms. Eur. Biophys. J. 25, 347–359.

Harding, S.E., Horton, J.C., and Johnson, P. (1997). (To be published.)

Iniesta, A., Diaz, F.G., and Garcia de la Torre, J. (1989). Transport properties of rigid bent-rod macromolecules and of semi-flexible broken rods in the rigid-body treatment: Analysis of the flexibility of of myosin rod. Biophys, J. 54, 269–276.

Johnsen, R.M. and Brown, W. (1992). An overview of current methods of analysing QLS data. In: *Laser Light Scattering in Biochemistry.* (Harding, S.E., Sattelle, D.B., and Bloomfield, V.A., Eds.), p. 77–91. Royal Society of Chemistry, Cambridge, England.

Johnson, P. (1984). Light-scattering and correlation-measurement. Biochem. Soc. Trans. 12, 623–625.

Johnson, P. and Mihalyi, E. (1965). Physicochemical studies of bovine fibrinogen. 2. Depolarization of fluorescence studies. Biochim. Biophys. Acta. 102, 476–486.

Jumel, K., Fiebrig, I, and Harding, S.E. (1996). Rapid size distribution and purity analysis of gastric mucus glycoproteins by size exclusion chromatography/multiangle laser light scattering. Int. J. Biol. Macromol. 18, 133–139.

Kratky, O., Leopold, H., and Stabinger, H. (1973). The determination of the partial specific volume of proteins by mechanical oscillator technique. Meth. Enzymol. 27D, 98–110.

Langley, K.H. (1992). Developments in electrophoretic laser light scattering and some biochemical applications. In: *Laser Light Scattering in Biochemistry* (Harding, S.E., Sattelle, D.B., and Bloomfield, V.A., Eds.), p.151–160. Royal Society of Chemistry, Cambridge, England.

Livesey, A.K. and Brochon, J. (1989). Maximum entropy data analysis of dynamic parameters from pulsed-fluorescent decays. In: *Dynamic Properties of Biomolecular Assemblies.* (Harding, S.E. and Rowe, A.J., Eds.), p.135. Royal Society of Chemistry, Cambridge, England.

Perkins, S.J. (1986). Protein volumes and hydration effects: The calculations of partial specific volumes, neutron-scattering match points and 280-nm absorption coefficients for proteins and glycoproteins from amino-acid sequences. Eur. J. Biochem. 157, 169–180.

Perkins, S.J. (1989). Hydrodynamic modelling of complement. In: Dynamic Properties of Biomolecular Assemblies (Harding, S.E. and Rowe, A.J., Eds.), p. 226–245. Royal Society of Chemistry, Cambridge, England.

Perkins, S.J. (1994). In: *Microscopy, Optical Spectroscopy and Macroscopic Techniques*. (Jones, C., Mulloy, B., and Thomas, A.H., Eds.), Vol. 22, p. 39. Humana Press, NJ.

Philo, J. (1994). Measuring sedimentation, diffusion, and molecular weights of small molecules by direct fitting of sedimentation velocity profiles. In: *Modern Analytical Ultracentrifugation*. (Schuster, T.M., and Laue, T.M., Eds.), p. 156–170. Birkhäuser, Boston.

Pörschke, D. and Antonsiewicz, J. (1989). Analysis of macromolecular structures in solution by electrooptical procedures. In: *Dynamic Properties of Biomolecular Assemblies*. (Harding, S.E. and Rowe, A.J., Eds.), p. 103–114. Royal Society of Chemistry, Cambridge, England.

Pörschke, D. and Obst, A. (1991). An electric field jump apparatus with ns time resolution for electrooptical measurements at physiological salt concentrations. Rev. Sci. Instrum. 62, 818–820.

Pusey, P.N. (1974). Macromolecular diffusion. In: *Photon Correlation and Light Beating Spectroscopy*. (Cummins, H.Z. and Pike, E.R., Eds.). p. 387–428, Plenum, New York.

Rholam, M. and Nicolas, P. (1981). Side-by-side dimerization of neurophysin: Sedimentation-velocity, viscometry, and fluorescence polarization studies. Biochemistry 20, 5837–5843.

Ridgeway, D. (1966). Transient electric birefringence of suspensions of asymmetric ellipsoids. J. Am. Chem. Soc. 88, 1104–1112.

Roark, D. and Yphantis, D.A. (1969). Studies of self-associating systems by equilibrium ultracentrifugation. Ann. N.Y. Acad. Sci. 164, 245–278.

Rowe, A.J. (1977). Concentration-dependence of transport processes—general description applicable to sedimentation, translational diffusion, and viscosity coefficients of macromolecular solutes. Biopolymers 16, 2595–2611.

Rowe, A.J. (1978). Techniques for determining molecular weight. Techn. Life Sci.: Biochem. B105a, 1–31.

Rowe, A.J. (1992). The concentration-dependence of sedimentation. In: *Analytical Ultracentrifugation in Biochemistry and Polymer Science*. (Harding, S.E., Rowe, A.J., and Horton, J.C., Eds.), p. 394–406. Royal Society of Chemistry, Cambridge, England.

Sanders, A.H. and Cannell, D.S. (1980). In: *Light Scattering in Liquids and Macromolecular Solutions*. (Degiorgio, V., Corti, M., and Giglio, M., Eds.), p. 173, Plenum, New York.

Schachman, H.K. (1989). Analytical ultracentrifugation reborn. Nature 341, 259–260.

Schachman, H.K., Pauza, C.D., Navre, M., Karela, M.J., Wu, L., and Yang, Y.R. (1984). Location of amino-acid alterations in mutants of aspartate transcarbamylase-structural aspects of interallelic complementation. Proc. Natl. Acad. Sci. USA, 81, 115–119.

Schmitz, K.S. (1990). *An Introduction to Dynamic Light Scattering by Macromolecules*. Academic Press, New York.

Schuster, T.M. and Laue, T.M. (Eds.)(1994). *Modern Analytical Ultracentrifugation*, Birkhäuser, Boston.

Stafford, W.F. (1992). Methods for obtaining sedimentation coefficient distributions. In: *Analytical Ultracentrifugation in Biochemistry and Polymer Science*. (Harding, S.E., Rowe, A.J., and Horton, J.C., Eds.) p. 359–393. Royal Society of Chemistry, Cambridge, England.

Štepánek, P. (1993). Data analysis in dynamic light scattering. In: *Dynamic Light Scattering. The Method and Some Applications*. (Brown, W., Ed.) Oxford University Press, Oxford, England.

Svedberg, T. and Pedersen, K.O. (1940). *The Ultracentrifuge*. Oxford University Press, Oxford, England.

Tanford, C. (1955). Intrinsic viscosity and kinematic viscosity. J. Phys. Chem. 59, 798–799.

Tanford, C. (1961). *Physical Chemistry of Macromolecules*. J. Wiley & Sons, New York.

Teller, D.C. (1973). Characterization of proteins by sedimentation equilibrium in the ultracentrifuge. Meth. Enzymol. 27D, 346–441.

Tombs, M.P. and Peacocke, A.R. (1974). *The Osmotic Pressure of Biological Macromolecules,* Oxford University Press, Oxford.

Van Holde, K.E. (1971). *Physical Biochemistry*. First ed. Prentice Hall, Englewood Cliffs, New Jersey.

Van Holde, K.E. (1985). *Physical Biochemistry.* Second ed. Prentice Hall, Englewood Cliffs, New Jersey.

Weber, G. (1952). Polarization of the fluorescence of macromolecules. I. Theory and experimental method. Biochem. J. 51, 145–155.

Weber, G. (1952). Polarization of the fluorescence of macromolecules. II. Fluorescent conjugates of ovalbumin and bovine serum albumin. Biochem. J. 51, 155–167.

Wells, C., Molina-Garcia, A.D., Harding, S.E. and Rowe, A.J. (1990). Self-interaction of dynein from *Tetrahymena* cilia. J. Mus. Res. Cell Motil. 11, 344–350.

Wyatt, P.J. (1992). In: *Laser Light Scattering in Biochemistry.* (Harding, S.E., Sattelle, D.B., Boomfield, V.A., Eds.), p. 35–58, Royal Society of Chemistry, Cambridge, England.

Yang, J.T. (1961). Viscosity of macromolecules in relation to molecular conformation. Adv. Prot. Chem. 16, 323–400.

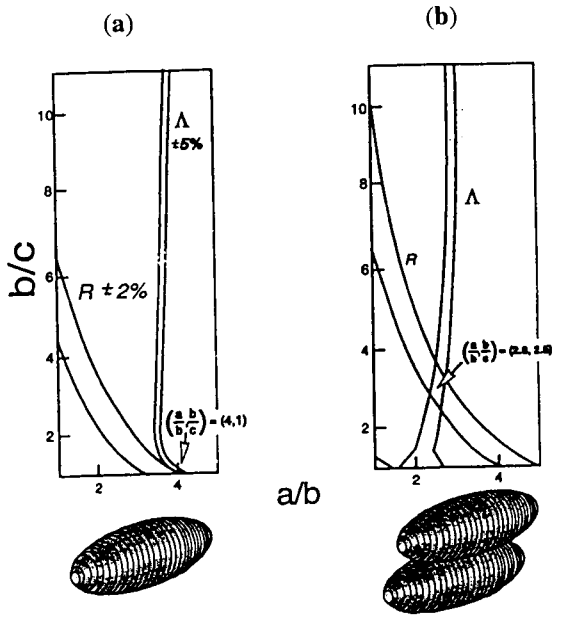

Figure 8. Triaxial ellipsoid gross conformation evaluations for (a) neurophysin monomers and (b) neurophysin dimers. Plots of constant values for Λ and R "line solutions" in the {a/b, b/c} plane. To perform these analyses, knowledge of three hydrodynamic parameters (for monomer and dimer) is required: $[\eta]$ (intrinsic viscosity), τ_h (from steady-state fluorescence depolarization), and k_s (from sedimentation velocity). Monomers: {a/b, b/c} = (4,1); Dimers: {a/b, b/c} = (2.8, 2.5). Redrawn and adapted from Harding and Rowe (1982b).

(Johnson and Mihalyi, 1965); finally, in the steady-state method described above, the use of solvents of differing T and η must cause no significant conformation change.

The harmonic mean itself is a mean over different rotational relaxation modes of the protein, each containing potential shape information. To resolve these requires a pulsed light source, time-resolved measurements, and mathematical algorithms for adequate deconvolution of the light source decay function and resolution of multiexponential terms, a by no means simple task (see, for example, Han et al., 1989; Livesey and Brochon, 1989). Electric birefringence (or dichroism) decay is, however, another attractive alternative to time-resolved fluorescence anisotropy decay measurements since, for a given isotropic monodisperse asymmetric scatterer, there are just two exponential to resolve (Ridgeway, 1966). A serious restriction of electrooptical methods, however, has been the restriction to solutions of low ionic strengths because of heating effects caused by the strong electric fields used.